IEEE Access
Multidisciplinary ⋮ Rapid Review ⋮ Open Access Journal

Received July 9, 2019, accepted July 19, 2019, date of publication July 23, 2019, date of current version December 2, 2019.

Digital Object Identifier 10.1109/ACCESS.2019.2930559

Open-Closed-Loop PD Iterative Learning Control Corrected With the Angular Relationship of Output Vectors for a Flexible Manipulator

JIAN DONG[1], BIN HE[1], MING MA[1,2], CHENGHONG ZHANG[1], AND GANG LI[1]
[1]College of Electronics and Information Engineering, Tongji University, Shanghai 201804, China
[2]Electric Power Research Institute, State Grid Gansu Electric Power Company, Lanzhou 730030, China

Corresponding authors: Bin He (hebin@tongji.edu.cn) and Ming Ma (283257683@qq.com)

This work was supported by the National Natural Science Foundation of China under Grant nos. 61801330, 61825303, 2018YFB1305300 and U1713215. It is was supported by Key innovation team program of innovation talents promotion plan by MOST of China (No. 2016RA4059), the Major Project of Gansu Province (17ZD2GA010) and National Key R&D Program of China 2017YFB0902200.

ABSTRACT A new iterative learning control (ILC) approach combined with an open-closed-loop PD scheme is presented for a flexible manipulator with a repeatable motion task in the case that only the endpoint pose of the flexible link is measurable. This approach takes advantage of the fact that the ILC performance is independent of the model used, thereby overcoming the drawback of the heavy reliance of PD controllers on the modeling accuracy. The open-closed-loop PD controller is mainly used to simultaneously reduce the effects of the modeling error and disturbances to enhance the controller's robustness. Meanwhile, an angular correction term is introduced by using the angular relationship of the system outputs to reward or penalize the ILC law. Specifically, when the current output tends toward the expected trajectory, the ILC law is enhanced accordingly; otherwise, it is penalized. The convergence conditions for the proposed approach are obtained through theoretical analysis, and experiments using a real flexible manipulator are presented. The results show that the proposed ILC scheme can overcome the impact of the endpoint error caused by link flexibility and has a good control effect.

INDEX TERMS Flexible manipulator, angular relationship, PD, open-closed-loop, iterative learning control.

I. INTRODUCTION

A flexible manipulator [1]–[3] consisting of light, flexible rods offers several advantages over traditional rigid manipulators [4]–[7], including a higher ratio of load to mass, lower inertia, and a faster system response. Thus, flexible manipulators have come to occupy an important position in the field of robotics, especially in recent years, and the study of flexible manipulators has received extensive attention in many fields. Using Hamilton's principle, Choi and Krishnamurthy [8] established a dynamic model of a flexible mechanical arm composed of one flexible bar and two rigid bars and discussed the nonlinear characteristics of the equation using mathematical tools. Damaren [9] proposed a combination of rigid positioning and flexible vibration that achieved a good control effect and applied this concept to develop a multilink flexible mechanical arm, which was verified through simulation and experimentation. Ulrich and Jurek [10] constructed a more accurate nonlinear flexible joint model and applied a design method based on singular perturbation theory to develop a flexible joint arm.

However, a flexible manipulator is a non-minimum-phase system with high nonlinearity and a high coupling uncertainty; consequently, trajectory tracking is very difficult. Together with the corresponding computational complexity and equipment cost, this is a disadvantage that hinders flexible robotic manipulators in performing jobs requiring a high accuracy and speed. Therefore, we propose a novel iterative learning control (ILC) scheme for the trajectory tracking of a flexible manipulator that can enable such a manipulator to follow an expected trajectory by means of iterative learning without requiring an accurate model. ILC [11]–[14] is a feed-forward control technique that improves the performance of a system performing repetitive tasks by reducing the tracking error from trial to trial. The basic idea behind an iterative algorithm is that a skill can be improved and ultimately

The associate editor coordinating the review of this manuscript and approving it for publication was Guangdeng Zong.

perfected through constant practice. The performance of systems that execute repetitive tasks can be improved by learning from previous executions. The concept of ILC was first presented by Arimoto *et al.* [15] in 1984, who proposed a learning control scheme called the improvement process, and since then, many researchers [16], [17] have addressed flexible manipulator control in combination with ILC. By using an iterative learning method, Qu [18] obtained the boundary control conditions for a flexible manipulator system. Gunnarsson *et al.* [19] used an ILC algorithm to estimate the angle of a flexible mechanical arm by measuring the motor angle and the angular acceleration of the arm. There are some other methods that we can learn from [20]–[23].

In this paper, a combination of ILC and open-closed-loop PD control is established. Iterative learning methods reduce the requirements for the system accuracy and can compensate for the inadequacy of a flexible manipulator model. Open-closed-loop PD [24]–[26] controllers can effectively reduce the uncertainty of the structure and parameters and the influence of unknown disturbances. Thus, a combination of the two can not only greatly reduce system error but also improve tracking accuracy over the entire working period. In addition, an angular correction term is introduced for the online adjustment of the gain coefficients of the open-closed-loop PD-ILC algorithm. Compared with traditional learning laws with a fixed learning gain, this approach allows further exploitation of the beneficial information contained in the system outputs, thereby improving the dynamic performance. The proposed algorithm improves the robustness and reduces the vibration of a flexible manipulator system.

This paper is organized as follows. In Section II, a dynamic model of a single-link flexible manipulator system is presented. In Section III, a novel ILC algorithm with an angular correction term is proposed. A convergence analysis is presented in Section IV. In Section V, a comparative experimental study is reported to verify the effectiveness of the proposed algorithm. Finally, conclusions are drawn in Section VI.

II. DYNAMIC MODEL OF A SINGLE-LINK FLEXIBLE MANIPULATOR

As shown in Fig. 1, under a direct-drive DC servomotor [27]–[29], a single-link flexible mechanical arm moves around the centerline of the motor rotor in the horizontal plane. One end is fixed to the motor rotor shaft, while the other end is loaded with a mass block. The fixed frame XOY is an inertial frame, and $X_P OY_P$ is a tangent frame, in which the OX_P axis is always tangent to the flexible arm at point O. The motion of the flexible arm in the horizontal plane can be described as the superposition of the motion of a rigid body over a large range and the motion of elastic deformation over a small range. The rigid angle of the flexible arm is represented by $\theta(t)$, and the amplitude of the superposed small elastic deformation varies with the position and time for each point along the arm. The elastic deformation at any point P on the arm at time t is expressed as $\omega(x, t)$, where x is the horizontal coordinate of P in the $X_P OY_P$ coordinate system.

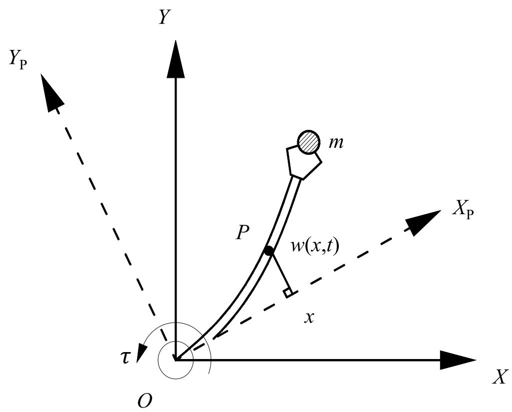

FIGURE 1. Schematic diagram of a single-link flexible mechanical arm.

The unit vector along the OX axis is i_0, the unit vector along the OY axis is j_0, the unit vector along the OX_P axis is i_P, and the unit vector along the OY_P axis is j_P; thus, the position vector of any point on the arm can be expressed as

$$OP = x_P i_P + y_P j_P = x_{Po} i_o + y_{Po} j_o \tag{1}$$

The velocity vector at P is

$$v_P \frac{dOP}{dt} = \frac{dx_P}{dt} i_P + \frac{dy_P}{dt} j_P = \frac{dx_{Po}}{dt} i_o + \frac{dy_{Po}}{dt} j_o \tag{2}$$

Under the assumption of no longitudinal deformation of the flexible arm, it may be stated that $\dot{x}_P = 0$, and the absolute speed at P is

$$v_P^2 = \left(x_P^2 + \omega^2(x,t)\right)\dot{\theta}^2(t) + \dot{\omega}^2(x,t) + 2x_P\theta^2(t)\,\omega^2(x,t) \tag{3}$$

where $\dot{\theta}$ is the speed of the rigid motion of the flexible arm and $\dot{\omega}(x,t)$ is the speed of the lateral deformation motion.

We use the Lagrangian equations [30]–[32] to establish a dynamic model of a single-link flexible arm. The total kinetic energy of the single-link flexible manipulator system is T, the kinetic energy of the motor rotor is T_1, and the kinetic energy of the flexible arm itself is T_2:

$$\begin{aligned} T &= T_1 + T_2 \\ T_1 &= I_r\dot{\theta}^2 \big/ 2 \end{aligned} \tag{4}$$

where I_r is the moment of inertia of the motor rotor with respect to the rotor centerline.

The kinetic energy of the flexible manipulator is

$$T_2 = \frac{1}{2}\rho A \int_0^l \left[\left(x^2 + \omega^2\right)\dot{\theta}^2 + \dot{\omega}^2 + 2x\dot{\theta}\dot{\omega}\right] dx \tag{5}$$

The elastic potential energy of the bending deformation is

$$V = \frac{1}{2} EI \int_0^l \left(\frac{\partial^2 \omega}{\partial x^2}\right)^2 dx \tag{6}$$

Using the small deformation hypothesis $\left(x^2 \gg \omega^2\right)$, $\omega = \sum_{k=1}^{\infty} \varphi_k(x)\, q_k(t)$ and the orthogonality of the modal functions, the simplified Lagrangian function is expressed as

$$L = \frac{1}{2}\left(I_r + \frac{\rho A l^3}{3}\right)\dot{\theta}^2 + \frac{1}{2}\rho A \sum_{k=1}^{\infty} \dot{q}_k^2(t) + \rho A \dot{\theta} \sum_{k=1}^{\infty} \dot{q}_k^2(t)\gamma_i - \frac{1}{2}\rho A \sum_{k=1}^{\infty} \dot{q}_k^2(t)\omega_i^2 \quad (7)$$

The work performed by the driving torque τ on the flexible arm is

$$G = \tau\theta(t) \quad (8)$$

where θ is a generalized coordinate and q_k ($q_k(t)$) corresponds to the generalized force:

$$F_\theta = \partial G/\partial\theta = \tau$$
$$F_{qk} = \partial G/\partial q_k = 0 \quad (9)$$

The Lagrangian equations of the flexible manipulator system are

$$\frac{d}{dt}\left(\frac{\partial L}{\partial\dot{\theta}}\right) - \frac{\partial L}{\partial\theta} = F_\theta$$
$$\frac{d}{dt}\left(\frac{\partial L}{\partial\dot{q}_k}\right) - \frac{\partial L}{\partial q_k} = F_{qk} \quad (10)$$

According to the above formulas, the dynamic equations for the single-link flexible mechanical arm in component form are

$$\ddot{q}_k(t) + \omega_k^2(x)\, q_k(t) + \gamma_k\ddot{\theta}(t) = 0$$
$$I_r\ddot{\theta}(t) + \rho S\sum_{k=1}^{\infty}\gamma_k\ddot{q}_k(t) = \tau \quad (11)$$

where S is the cross-sectional area of the rod, ρ is the volume density, $q_k(t)$ represents the elastic mode coordinates, $\omega_k(x)$ are the modal functions, γ_k are the position vectors of the arm, τ is the driving torque acting on the flexible mechanical arm, I_r is the moment of inertia of the motor rotor with respect to the rotor centerline, $\ddot{\theta}(t)$ is the angular acceleration of the rigid body motion, t is the time variable, and k is the order of the equation.

The single-link flexible arm is taken as the control object, and the state vector $x(t)$ is taken to be

$$x(t) = \left[\theta(t), \dot{\theta}(t), q_1(t), \dot{q}_1(t), \cdots, q_k(t), \dot{q}_k(t), \cdots\right]^T \quad (12)$$

where $\dot{q}_k(t)$ is the elastic mode speed.

The complete state-space expression for the flexible mechanical arm is

$$\begin{cases}\dot{x}(t) = Ax(t) + Bu(t) \\ y(t) = Cx(t)\end{cases} \quad (13)$$

where A, B and C are corresponding matrices, $x(t)$ is the state vector of the system, $u(t)$ is the input to the system, and $y(t)$ is the output of the system (the end position of the flexible manipulator).

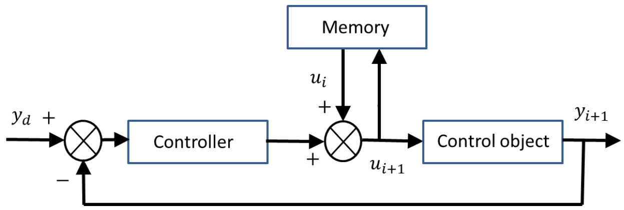

FIGURE 2. Diagram of the ILC system.

III. DESIGNED ILC ALGORITHM WITH AN ANGULAR CORRECTION TERM

The control algorithm designed in this paper can be expressed as

$$u_{i+1}(t) = u_i(t) + (1+\cos\beta_i)\left[\varphi_2(t)\dot{e}_i(t) + \Psi_2(t)e_i(t)\right] + (1+\cos\beta_{i+1})\left[\varphi_1(t)\dot{e}_{i+1}(t) + \Psi_1(t)e_{i+1}(t)\right] \quad (14)$$

where i denotes the iteration number; $\varphi_1(t)$, $\varphi_2(t)$, $\Psi_1(t)$ and $\Psi_2(t)$ are the learning gain matrices; and $e_i(t) = y_d(t) - y_i(t)$. A system block diagram of the iterative learning controller designed based on the simplified model derived in this paper is shown in Fig. 2.

The aim of ILC is to find the ideal control input $u_d(t)$ for the system by modifying the control quantity such that the output $y_d(t)$ exactly tracks the desired output. Since the expected input is unknown, there is no standard reference for whether the system input is good or bad in each iteration; only the output can reveal the quality of the input. Although the general ILC algorithm uses the output deviations to correct the input, this approach is subject to considerable blindness. Therefore, we also impose a special coefficient on the ILC law to determine an appropriate reward or punishment for the control law in accordance with its effect. When the system output $y_i(t)$ is close to the expected output $y_d(t)$, the corresponding ILC correction can be enhanced through this coefficient. When the system output $y_i(t)$ deviates from the expected output $y_d(t)$, the ILC correction can be weakened. In this paper, we consider not only the error between the system output and the reference trajectory but also the spatial orientation relationship among the three variables in the output vector space.

As shown in Fig. 3, the vector $\vec{OA}$ represents the expected trajectory $y_d(t)$, the vector $\vec{OB}$ represents the output $y_i(t)$ in the i-th iteration, and the vector $\vec{OC}$ represents the output $y_{i+1}(t)$ in the $i+1$-th iteration; thus, the vector $\vec{BA}$ represents the error $e_i(t) = y_d(t) - y_i(t)$ in the $i+1$-th iteration. The desired output trajectory is constant, and the purpose of the iterative process is to make $y_i(t)$ gradually approach $y_d(t)$. The error $e_i(t)$ is the error in the i-th iteration. It is believed that when the direction of development of the output in the $i+1$-th iteration lies above the dotted line BD, the correction of the input should be strengthened, whereas if the opposite

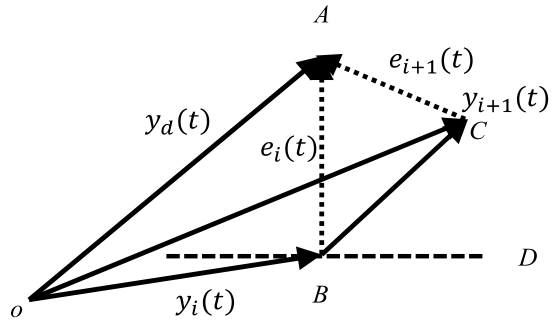

FIGURE 3. Angular relationship in the output vector space.

is true, it should be weakened. Let us set $\angle ABC = \beta_i$.

$$\cos\beta_i = \frac{e_i(t)\left(y_{i+1}(t) - y_i(t)\right)}{\|e_i(t)\|\,\|y_{i+1}(t) - y_i(t)\|}$$
$$\cos\beta_{i+1} = \frac{e_{i+1}(t)\left(y_{i+2}(t) - y_{i+1}(t)\right)}{\|e_{i+1}(t)\|\,\|y_{i+2}(t) - y_{i+1}(t)\|} \tag{15}$$

The above expressions serve as a basis for judging the quality of the ILC law based on vector analysis. When $\cos\beta_i < \pi/2$, the correction should be strengthened, which is equivalent to the reward for the ILC law discussed previously. The correction will be continuously enhanced with the decreasing β_i. When $\beta_i = 0$, the reward is the largest. When $\cos\beta_i > \pi/2$, the modification should be weakened, which is equivalent to the punishment of the ILC law discussed previously. When $\beta_i = \pi$, the correction is completely eliminated; that is, the penalty reaches its maximum.

IV. CONVERGENCE ANALYSIS

The complete state-space expression for the single-link flexible mechanical system is

$$\begin{cases} \dot{x}_i(t) = f(x_i, t) + B(t)u_i(t) + \omega_i(x_i, t) \\ y_i(t) = C(t)x_i(t) + \nu_i(t) \end{cases} \tag{16}$$

where i and t are the iteration number and the run time, respectively; $x_i \in R^m$ is the state variable, while $u_i(t) \in R^m$ is the control variable; $y_i(t) \in R^m$ is the system output; $\omega_i(t)$ and $\nu_i(t)$ are the uncertainty term and interferential term, respectively; and $f(\cdot)$, $B(\cdot)$, and $w(\cdot)$ are functions.

Assumption 1: Functions f and ω are uniformly Lipschitz with respect to x, $\Omega \in R^m \times R^m \times [1, T]$,

$$\|f(x_{i+1}, t) - f(x_i, t)\| \le k_f \|x_{i+1} - x_i\|$$
$$\|\omega(x_{i+1}, t) - \omega(x_i, t)\| \le k_\omega \|x_{i+1} - x_i\| \tag{17}$$

where $k_f > 0$ and $k_\omega > 0$ are the Lipschitzian constants.

Assumption 2: The control input matrix $C(t)$ is first-order differentiable and continuous, and $B(t)$ and $C(t)$ exist.

Assumption 3: There exist a $u_d(t)$ and an $x_d(t)$ that make the desired trajectory $y_d(t)$ first-order differentiable and continuous.

Assumption 4: The initial value of the system satisfies the following criterion:

$$\|x_{i+1}(0) - x_i(0)\| \le b_{x_0}, \quad \forall i \tag{18}$$

Theorem: Under the action of the ILC algorithm (14), the convergence conditions for the system are

$$\rho_1 = \max_{t\in[0,T]} \|I + \varphi_1(t)(1 + \cos\beta_{i+1})B(t)C(t)\|^{-1} < 1$$
$$\rho_2 = \max_{t\in[0,T]} \|I - \varphi_2(t)(1 + \cos\beta_i)B(t)C(t)\| < 1 \tag{19}$$

Then, the tracking error bound converges to within a small neighborhood of the origin, and we can conclude that $y_i(t) \to y_d(t)\ (i \to \infty)$.

Let us define the following variables:

$$\Delta x_i(t) = x_d(t) - x_i(t)$$
$$\Delta u_i(t) = u_d(t) - u_i(t)$$
$$\Delta f_i(t) = f_d(t, x_d(t)) - f_i(t, x_i(t)) \tag{20}$$

where $x_d(t)$ is the state input on the desired trajectory and $u_d(t)$ is the control input on the desired trajectory.

Proof: From (16) and (20), the system output error can be obtained as follows:

$$e_i(t) = y_d(t) - y_i(t) = C(t)x_d(t) - C(t)x_i(t)$$
$$= C(t)\Delta x_i(t) - \nu_i(t) \tag{21}$$

The derivative of (21) can be expressed as

$$\dot{e}_i(t) = C(t)\Delta\dot{x}_i(t) + \dot{C}(t)\Delta x_i(t) - \dot{\nu}_i(t) \tag{22}$$

From (14), we obtain

$$\begin{aligned}\Delta u_{i+1}(t) = \Delta u_i(t) &- \varphi_1(t)(1 + \cos\beta_{i+1})\dot{e}_{i+1}(t) \\ &- \varphi_2(t)(1 + \cos\beta_i)\dot{e}_i(t) \\ &- \Psi_1(t)(1 + \cos\beta_{i+1})e_{i+1}(t) \\ &- \Psi_2(t)(1 + \cos\beta_i)e_i(t)\end{aligned} \tag{23}$$

Substituting (22) into (23) yields

$$\begin{aligned}&\Delta u_{i+1}(t) \\ &= \Delta u_i(t) - \Psi_1(t)(1 + \cos\beta_{i+1})C(t)\Delta x_{i+1}(t) \\ &\quad - \varphi_1(t)(1 + \cos\beta_{i+1})[C(t)\Delta\dot{x}_{i+1}(t) \\ &\quad + \dot{C}(t)\Delta x_{i+1}(t) - \dot{\nu}_{i+1}(t)] \\ &\quad - \varphi_2(t)(1+\cos\beta_i)\left[C(t)\Delta\dot{x}_i(t) + \dot{C}(t)\Delta x_i(t) - \dot{\nu}_i(t)\right] \\ &\quad - \Psi_2(t)(1 + \cos\beta_i)C(t)\Delta x_i(t) \\ &\quad + \Psi_1(t)(1+\cos\beta_{i+1})\nu_{i+1}(t) + \Psi_2(t)(1+\cos\beta_i)\nu_i(t)\end{aligned} \tag{24}$$

From (16) and (20), we obtain

$$\Delta\dot{x}_i(t) = \Delta f_i(t) + B(t)\Delta u_i(t) + \Delta\omega_i(t)$$
$$\Delta\dot{x}_{i+1}(t) = \Delta f_{i+1}(t) + B(t)\Delta u_{i+1}(t) + \Delta\omega_{i+1}(t) \tag{25}$$

Substituting (25) into (24) yields

$$\begin{aligned}&[I + (1 + \cos\beta_{i+1})\varphi_1(t)C(t)B(t)]\Delta u_{i+1}(t) \\ &= [I - \varphi_2(t)(1 + \cos\beta_i)C(t)B(t)]\Delta u_i(t) \\ &\quad - \varphi_1(t)(1+\cos\beta_{i+1})\left[C(t)\Delta f_{i+1}(t) + \dot{C}(t)\Delta x_{i+1}(t)\right] \\ &\quad - \varphi_2(t)(1 + \cos\beta_i)\left[C(t)\Delta f_i(t) + \dot{C}(t)\Delta x_i(t)\right]\end{aligned}$$

$$
\begin{aligned}
&-\Psi_1(t)(1+\cos\beta_{i+1})C(t)\Delta x_{i+1}(t)\\
&-\Psi_2(t)(1+\cos\beta_i)C(t)\Delta x_i(t)\\
&+\varphi_1(t)(1+\cos\beta_{i+1})(\dot{v}_{i+1}(t)-\Delta\omega_{i+1}(t))\\
&+\varphi_2(t)(1+\cos\beta_i)(\dot{v}_i(t)-\Delta\omega_i(t))\\
&+\Psi_1(t)(1+\cos\beta_{i+1})v_{i+1}(t)+\Psi_2(t)(1+\cos\beta_i)v_i(t)
\end{aligned} \tag{26}
$$

According to **Assumption 1**, we obtain

$$\|\Delta f_i(t)\| \le k_f\|\Delta x_i(t)\| \tag{27}$$

Taking the λλ-norm, we can obtain

$$
\begin{aligned}
&\|\Delta u_{i+1}(t)\|_\lambda\\
&\le \eta_1\eta_2\|\Delta u_i(t)\|_\lambda\\
&\quad+\eta_1\left[P_{d1}k_fP_{C2}+P_{d1}P_{C1}+P_{P1}P_{C2}\right]\|\Delta x_{i+1}(t)\|_\lambda\\
&\quad+\eta_1\left[k_fP_{d2}P_{C2}+P_{d2}P_{C1}+P_{P2}P_{C2}\right]\|\Delta x_i(t)\|_\lambda\\
&\quad+\eta_1\left[(P_{d1}+P_{d2})(b_{cv}-b_\omega)+(P_{P1}+P_{P2})b_v\right]
\end{aligned} \tag{28}
$$

where

$$
\begin{aligned}
\eta_1 &= \|I+\varphi_1(t)(1+\cos\beta_{i+1})C(t)B(t)\|^{-1},\\
\eta_2 &= \|I-\varphi_2(t)(1+\cos\beta_i)C(t)B(t)\|,\\
P_{C1} &= \max_{t\in[0,T]}\|\dot{C}(t)\|,\\
P_{d1} &= \max_{t\in[0,T]}\|\varphi_1(t)(1+\cos\beta_{i+1})\|,\\
P_{C2} &= \max_{t\in[0,T]}\|C(t)\|,\\
P_{d2} &= \max_{t\in[0,T]}\|\varphi_2(t)(1+\cos\beta_i)\|,\\
P_{P2} &= \max_{t\in[0,T]}\|\Psi_2(t)(1+\cos\beta_i)\|,\\
P_{P1} &= \max_{t\in[0,T]}\|\Psi_1(t)(1+\cos\beta_{i+1})\|,\\
b_v &= \max_{t\in[0,T]}\{\sup\|v_i(t)\|,\sup\|v_{i+1}(t)\|\},\\
b_{cv} &= \max_{t\in[0,T]}\{\sup\|\dot{v}_i(t)\|,\sup\|\dot{v}_{i+1}(t)\|\},\ \text{and}\\
b_\omega &= \max_{t\in[0,T]}\{\sup\|\omega_i(t)\|,\sup\|\omega_{i+1}(t)\|\}.
\end{aligned}
$$

From (16), the state vector $x_i(t)$ can be written as

$$x_i(t)=\int_0^1[f(x_i(\tau),\tau)+B(\tau)u_i(\tau)+\omega_i(x_i(\tau),\tau)]d\tau+x_i(0) \tag{29}$$

The expected state vector of the system can be written as

$$x_d(t)=\int_0^1[f(x_d(\tau),\tau)+B(\tau)u_d(\tau)+\omega_d(x_d(\tau),\tau)]d\tau+x_d(0) \tag{30}$$

By combining (29) and (30), we obtain

$$\Delta x_i(t)=\int_0^1[\Delta f_i(\tau)+B(\tau)\Delta u_i(\tau)+\Delta\omega_i(\tau)]d\tau+\Delta x_i(0) \tag{31}$$

According to **Assumptions 3** and **4**, taking the norm on both sides of (31) yields

$$\|\Delta x_i(t)\|=\int_0^1\left[k_f\|\Delta x_i(\tau)\|+\|B(\tau)\Delta u_i(\tau)\|+k_\omega\|\Delta x_i(\tau)\|\right]d\tau \tag{32}$$

According to the definition of the λ-norm, we set $\lambda > k_f + k_\omega$ and obtain

$$\|\Delta x_i(t)\|_\lambda \le \frac{P_B}{\lambda-k_f-k_\omega}\|\Delta u_i(t)\|_\lambda \tag{33}$$

where $P_B=\max_{t\in[0,T]}\|B(t)\|$.

Similarly,

$$\|\Delta x_{i+1}(t)\|_\lambda \le \frac{P_B}{\lambda-k_f-k_\omega}\|\Delta u_{i+1}(t)\|_\lambda \tag{34}$$

Applying (33) and (34) to (28), we obtain

$$
\begin{aligned}
&\left[1-\frac{\eta_1P_B(P_{d1}MP_{C2}+P_{d1}P_{C1}+P_{P1}P_{C2})}{\lambda-k_f-k_\omega}\right]\|\Delta u_{i+1}(t)\|_\lambda\\
&=\left[\eta_1\eta_2+\frac{\eta_1P_B(MP_{d2}P_{C2}+P_{d2}P_{C1}+P_{P2}P_{C2})}{\lambda-k_f-k_\omega}\right]\\
&\quad\times\|\Delta u_i(t)\|_\lambda+\kappa
\end{aligned} \tag{35}
$$

where $\kappa=\eta_1[(P_{d1}+P_{d2})(b_{cv}-b_\omega)+(P_{P1}+P_{P2})b_v]$.

From (35), we obtain

$$\|\Delta u_{i+1}(t)\|_\lambda \le \tilde{\rho}\|\Delta u_i(t)\|_\lambda+\xi \tag{36}$$

where $\tilde{\rho}=\frac{\eta_1\eta_2(\lambda-k_f-k_\omega)+\eta_1P_B(k_fP_{d2}P_{C2}+P_{d2}P_{C1}+P_{P2}P_{C2})}{\lambda-k_f-k_\omega-\eta_1P_B(P_{d1}k_fP_{C2}+P_{d1}P_{C1}+P_{P1}P_{C2})}$ and $\xi=\frac{\kappa(\lambda-k_f-k_\omega)}{\lambda-k_f-k_\omega-\eta_1P_B(P_{d1}k_fP_{C2}+P_{d1}P_{C1}+P_{P1}P_{C2})}$.

We set $\tilde{\rho}<1$; then,

$$0<\frac{\eta_1\eta_2(\lambda-k_f-k_\omega)+\eta_1P_B(k_fP_{d2}P_{C2}+P_{d2}P_{C1}+P_{P2}P_{C2})}{\lambda-k_f-k_\omega-\eta_1P_B(P_{d1}k_fP_{C2}+P_{d1}P_{C1}+P_{P1}P_{C2})}<1 \tag{37}$$

According to the previous assumption $\lambda > k_f + k_\omega$, we obtain

$$\eta_1\eta_2<1-\frac{\eta_1P_B(P_{d1}k_fP_{C2}+P_{d1}P_{C1}+P_{P1}P_{C2})}{\lambda-k_f-k_\omega}+\frac{\eta_1P_B(k_fP_{d2}P_{C2}+P_{d2}P_{C1}+P_{P2}P_{C2})}{\lambda-k_f-k_\omega} \tag{38}$$

According to the norm definition given in (28), we obtain

$$\eta_1P_B(P_{d1}MP_{C2}+P_{d1}P_{C1}+P_{P1}P_{C2})+\eta_1P_B(MP_{d2}P_{C2}+P_{d2}P_{C1}+P_{P2}P_{C2})>0 \tag{39}$$

Because $\eta_1\eta_2<1$, we obtain

$$\lim_{i\to\infty}\|\Delta u_i(t)\|_\lambda \le \xi/(1-\tilde{\rho}) \tag{40}$$

Substituting (40) into (34), we obtain

$$\lim_{i\to\infty}\|\Delta x_i(t)\|_\lambda \le \xi/(1-\tilde{\rho}) \tag{41}$$

FIGURE 4. Single-link planar flexible robotic manipulator.

From (34), we obtain

$$\lim_{i\to\infty} \|\Delta e_i(t)\|_\lambda \leq \xi \big/ (1-\tilde{\rho}) \tag{42}$$

Consequently, we find that if the condition $\eta_1\eta_2 < 1$ holds, then the tracking error bound converges to within a small neighborhood of the origin, and we can conclude that $y_i(t) \to y_d(t)\ (i \to \infty)$.

V. EXPERIMENT

To verify the feasibility and effectiveness of the ILC algorithm, we conducted an experimental study. The single-link planar flexible arm used in the experiments is shown in Fig. 4. The whole flexible arm is fixed to the base; the arm is composed of a light alloy material, the end of the arm is equipped with a clamping hand with a powerful sensor, and the joint is equipped with an encoder to detect the angular displacement. The desired reference trajectory for the flexible mechanical arm was defined as $q(t) = \left[\sin\left(\pi/3\right)t\right]$. The mechanical parameters of the flexible manipulator are shown in Table 1.

TABLE 1. Mechanical parameters of the flexible manipulator.

Description	Value	Unit
Connecting rod diameter	0.5	cm
Connecting rod length	0.48	m
Connecting rod density	0.45	kg/m
Moment of inertia of the joint	0.17	kg•m^2
Load mass	0.1	kg
Moment of inertia of the mass	0.021	kg•m^2

It is easy to verify that the end point trajectory approached the desired trajectory as the iterative learning process proceeded. Fig. 5 illustrates the trajectory tracking process in the experiment, and it is clear from these images how the iterative learning process recovered from the offset due to the flexibility of the link, showing that it is possible for the proposed controller to successfully cope with the difficult problem of trajectory tracking. Fig. 6 clearly shows the effectiveness of the open-closed-loop PD-ILC scheme with the angle correction term in terms of the tracking error reduction and resistance to disturbances. Fig. 7 presents the maximum tracking errors from one iteration to the next under ILC. These plots clearly demonstrate that the proposed algorithm can ensure lower tracking errors and faster convergence rates in comparison with the traditional open-closed-loop PD-ILC. These results strongly illustrate the importance of the angular correction term. During the last iteration, the system had an acceptably small tracking error due to the nonminimum phase of the flexible arm.

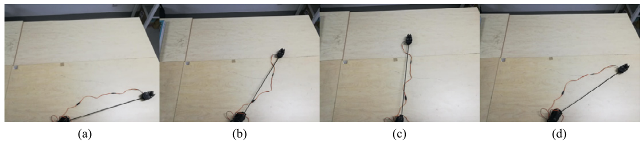

FIGURE 5. Trajectory movement of the flexible robotic arm with a load.

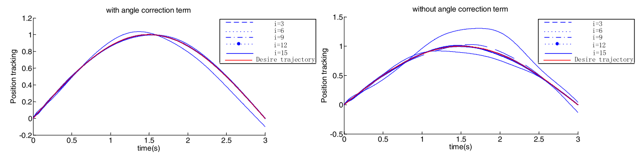

FIGURE 6. Trajectory tracking of the flexible arm during the process of iterative operation.

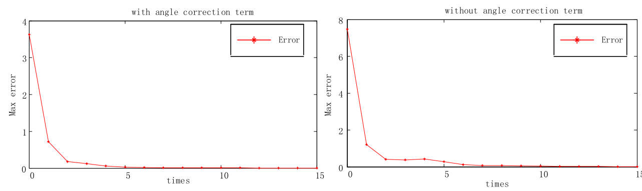

FIGURE 7. Maximum absolute tracking error in each iteration.

VI. CONCLUSION

A control algorithm based on open-closed-loop PD-ILC corrected with the angular relationship of the output vectors, which can take full advantage of the error information and achieve self-adjustment based on the output angular relationship, has been developed for a single-link flexible manipulator. Through experiments, we have found that in the presence of disturbances and uncertainties, the algorithm can still achieve accurate trajectory tracking and has a high anti-interference ability. The algorithm has a simple structure and is easy to implement in real systems. In the future, we will apply this algorithm in other control fields.

ACKNOWLEDGMENT

This work was supported by the National Natural Science Foundation of China under Grant nos. 61801330, 61825303, 2018YFB1305300 and U1713215. It is was supported by Key innovation team program of innovation talents promotion plan by MOST of China (No. 2016RA4059), the Major

Project of Gansu Province (17ZD2GA010) and National Key R&D Program of China 2017YFB0902200.

REFERENCES

[1] Q. Xu, Z. Jing, and S. Hu, "Research on the dynamic coupling of the rigid-flexible manipulator," *Int. J. Non-Linear Mech.*, vol. 103, pp. 27–36, 2018.

[2] Z.-C. Qiu and Z.-L. Zhao, "Vibration suppression of a pneumatic drive flexible manipulator using adaptive phase adjusting controller," *J. Vibrat. Control*, vol. 21, no. 15, pp. 2959–2980, 2015.

[3] H. Yang, Y. Yu, Y. Yuan, and X. Fan, "Back-stepping control of two-link flexible manipulator based on an extended state observer," *Adv. Space Res.*, vol. 56, no. 10, pp. 2312–2322, 2015.

[4] Z. Ma and G. Sun, "Dual terminal sliding mode control design for rigid robotic manipulator," *J. Franklin Inst.*, vol. 355, no. 18, pp. 9127–9149, 2017.

[5] Y.-S. Lu and Y.-Y. Lin, "Smooth motion control of rigid robotic manipulators with constraints on high-order kinematic variables," *Mechatronics*, vol. 49, pp. 11–25, Feb. 2018.

[6] V. Kumar and K. P. S. Rana, "Nonlinear adaptive fractional order fuzzy PID control of a 2-link planar rigid manipulator with payload," *J. Franklin Inst.*, vol. 354, no. 2, pp. 993–1022, 2017.

[7] R. Fareh, M. Saad, M. Saad, and M. Bettayeb, "Tracking trajectory in the workspace of rigid manipulators using distributed adaptive control strategy," *Adv. Robot.*, vol. 30, no. 6, pp. 1–13, 2016.

[8] B.-O. Choi and K. Krishnamurthy, "Unconstrained and constrained motion control of a planar two-link structurally flexible robotic manipulator," *J. Robot. Syst.*, vol. 11, no. 6, pp. 557–571, l994.

[9] C. J. Damaren, "Passivity analysis for flexible multilink space manipulators," *J. Guid. Control Dyn.*, vol. 18, no. 2, pp. 272–279,1995.

[10] S. Ulrich, J. Z. Sasiadek, and I. Barkana, "Modeling and direct adaptive control of a flexible-joint manipulator," *J. Guid., Control, Dyn*, vol. 35, no. 1, pp. 25–39, 2012.

[11] S. Sun, T. Endo, and F. Matsuno, "Iterative learning control based robust distributed algorithm for non-holonomic mobile robots formation," *IEEE Access*, vol. 6, pp. 61904–61917, 2018.

[12] T. Glück, M. Blank, D. Büchl, and A. Kugi, "Convex constrained iterative learning control using projection: Application to a smart power switch," *IEEE Trans. Control Syst. Technol.*, vol. 26, no. 5, pp. 1818–1825, Sep. 2018.

[13] T. Meng and W. He, "Iterative learning control of a robotic arm experiment platform with input constraint," *IEEE Trans. Ind. Electron.*, vol. 65, no. 1, pp. 664–672, Jan. 2018.

[14] Q. Yan, J. Cai, L. Wu, and Q. Zhou, "Error-tracking iterative learning control for nonlinearly parametric time-delay systems with initial state errors," *IEEE Access*, vol. 6, pp. 12167–12174, 2018.

[15] S. Arimoto, S. Kawamura, and F. Miyazaki, "Bettering operation of robots by learning," *J. Robot. Syst.*, vol. 1, no. 2, pp. 123–140, 1984.

[16] L. Zhang and S. Liu, "Basis function based adaptive iterative learning control for flexible manipulator," in *Proc. 11th World Congr. Intell. Control Automat. (WCICA)*, Shenyang, China, Jun./Jul. 2014, pp. 828–833.

[17] D. Mute, S. Ghosh, and B. Subudhi, "Iterative learning control of a single-link flexible manipulator based on an identified adaptive NARX model," in *Proc. Annu. IEEE India Conf. (INDICON)*, Mumbai, India, Dec. 2013, pp. 1–4.

[18] Z. Qu, "An iterative learning algorithm for boundary control of a stretched moving string," *Automatica*, vol. 38, pp. 821–827, May 2002.

[19] S. Gunnarsson, M. Norrlöf, E. Rahic, and M. Özbek, "On the use of accelerometers in iterative learning control of a flexible robot arm," *Int. J. Control J.*, vol. 80, no. 3, pp. 363–373, 2007.

[20] G. Zong, H. Ren, and L. Hou, "Finite-time stability of interconnected impulsive switched systems," *IET Control Theory Appl.*, vol. 10, no. 6, pp. 648–654, 2016.

[21] D. Yang, G. Zong, and H. R. Karimi, "H_∞ refined anti-disturbance control of switched LPV systems with application to aero-engine," *IEEE Trans. Ind. Electron.*, to be published, doi: 10.1109/TIE.2019.2912780.

[22] H. Ren, G. Zong, and T. Li, "Event-triggered finite-time control for networked switched linear systems with asynchronous switching," *IEEE Trans. Syst., Man, Cybern., Syst.*, vol. 48, no. 11, pp. 1874–1884, Jan. 2018.

[23] H. Ren, G. Zong, and H. R. Karimi, "Asynchronous finite-time filtering of networked switched systems and its application: An event-driven method," *IEEE Trans. Circuits Syst. I, Reg. Papers*, vol. 66, no. 1, pp. 391–402, Jan. 2019.

[24] Y. Hu, B. Zuo, and J. Li, "Fast algorithm of open-closed loop PD-type iterative learning control for DC motor," in *Proc. 6th World Congr. Intell. Control Automat. (WCICA)*, Jun. 2006, pp. 3834–3838.

[25] Z. Feng, Z. Zhang, and D. Pi, "Open-closed-loop PD-type iterative learning controller for nonlinear systems and its convergence," in *Proc. 5th World Congr. Intell. Control Automat. (WCICA)*, Jun. 2004, pp. 1241–1245.

[26] S.-J. Yu, J.-H. Wu, and X.-W. Yan, "A PD-type open-closed-loop iterative learning control and its convergence for discrete systems," in *Proc. Int. Conf. Mach. Learn. Cybern.*, vol. 2, 2002, pp. 659–662.

[27] O. Salas-Peña, H. Castañeda, and J. D. León-Morales, "Robust adaptive control for a DC servomotor with wide backlash nonlinearity," *Automatika*, vol. 56, no. 4, pp. 436–442, 2015.

[28] S. Saxena and Y. V. Hote, "Design and validation of fractional-order control scheme for DC servomotor via internal model control approach," *IETE Tech. Rev.*, vol. 36, no. 1, pp. 49–60, 2019.

[29] S. Khadraoui, H. Nounou, M. Nounou, A. Datta, and S. P. Bhattacharyya, "A model-free design of reduced-order controllers and application to a DC servomotor," *Automatica*, vol. 50, no. 8, pp. 2142–2149, 2014.

[30] F. Wang, S. Li, and Y. Zou, "A relationship between linear stability and index of oscillations for Lagrangian equation at higher order zones," *Nonlinear Anal., Real World Appl.*, vol. 47, pp. 178–187, Jun. 2019.

[31] G. Badin, M. Oliver, and S. Vasylkevych, "Geometric Lagrangian averaged Euler–Boussinesq and primitive equations," *J. Phys. A, Math. Theor.*, vol. 51, no. 45, 2018, Art. no. 455501.

[32] M. Zhang, X. Cen, and X. Cheng, "Linearized stability and instability of nonconstant periodic solutions of Lagrangian equations," *Math. Methods Appl. Sci.*, vol. 41, no. 12, pp. 4853–4866, 2018.

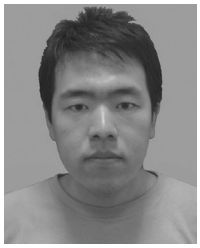

JIAN DONG was born in Harbin, China, in 1990. He is currently pursuing the Ph.D. degree with the Department of Control Science and Engineering, College of Electronics and Information Engineering, Tongji University. His current research interest includes the dynamics and control of robotic systems.

BIN HE received the B.S. degree in engineering machinery from Jilin University, Changchun, China, in 1996, and the Ph.D. degree in mechanical and electronic control engineering from Zhejiang University, Hangzhou, China, in 2001.

From 2001 to 2003, he held postdoctoral research appointments with the State Key Laboratory of Fluid Power Transmission and Control, Zhejiang University. He is currently a Professor with the Department of Control Science and Engineering, College of Electronics and Information Engineering, Tongji University, Shanghai, China. His current research interests include intelligent robot control, neural networks, biomimetic microrobots, image processing and fusion, wireless communication, and wireless networks.

Dr. He is an Associate Editor of *Neurocomputing*.

MING MA was born in Gansu, China, in February 1983. He received the M.E. degree from Zhejiang University, Hangzhou, China, in 2011. He is currently pursuing the Ph.D. degree with Tongji University. He is also with the Electric Power Research Institute, State Grid Gansu Electric Power Company. His research interests include the control of renewable energy generator systems, the technology of renewable energy integration, security and stability of power systems, and processing large data about renewable energy grid-connected operation control.

CHENGHONG ZHANG was born in February 1981. He received the B.S. degree from the Hunan University of Technology, in 2005, and the M.S. degree from Harbin Engineering University, in 2005. He is currently pursuing the Ph.D. degree with the Department of Control Science and Engineering, Tongji University. The research direction is soft robot system theory and intelligent control. His research interests include the research of soft robot design theory and method, actuator characteristics and electromechanical coupling model, control methods, and the related application.

GANG LI received the B.S. degree in measuring and control technology and instrumentations from China Jiliang University, in 2010, and the M.S. degree in control theory and control engineering and the Ph.D. degree in control science and engineering from Tongji University, China, in 2013 and 2018, respectively. He is currently an Assistant Research Fellow with the Department of Control Science and Engineering, College of Electronics and Information Engineering, Tongji University. His current research interests include intelligent sensing and wireless sensor networks.